

---

# IQAGPT: Image Quality Assessment with Vision-language and ChatGPT Models\*

---

**Zhihao Chen**<sup>†</sup>      **Bin Hu**<sup>†</sup>      **Chuang Niu**<sup>†</sup>      **Tao Chen**  
ISTBI      Huashan Hospital      BME & CBIS      ISTBI  
Fudan University      Fudan University      Rensselaer Polytechnic Institute      Fudan University

**Yuxin Li**<sup>‡</sup>      **Hongming Shan**<sup>‡</sup>      **Ge Wang**<sup>‡</sup>  
Huashan Hospital      ISTBI      BME & CBIS  
Fudan University      Fudan University      Rensselaer Polytechnic Institute

## Abstract

Large language models (LLMs), such as ChatGPT, have demonstrated impressive capabilities in various tasks and attracted an increasing interest as a natural language interface across many domains. Recently, large vision-language models (VLMs) like BLIP-2 and GPT-4 have been intensively investigated, which learn rich vision-language correlation from image-text pairs. However, despite these developments, the application of LLMs and VLMs in image quality assessment (IQA), particularly in medical imaging, remains to be explored, which is valuable for objective performance evaluation and potential supplement or even replacement of radiologists' opinions. To this end, this paper introduces IQAGPT, an innovative image quality assessment system integrating an image quality captioning VLM with ChatGPT for generating quality scores and textual reports. First, we build a CT-IQA dataset for training and evaluation, comprising 1,000 CT slices with diverse quality levels professionally annotated. To better leverage the capabilities of LLMs, we convert annotated quality scores into semantically rich text descriptions using a prompt template. Second, we fine-tune the image quality captioning VLM on the CT-IQA dataset to generate quality descriptions. The captioning model fuses the image and text features through cross-modal attention. Third, based on the quality descriptions, users can talk with ChatGPT to rate image quality scores or produce a radiological quality report. Our preliminary results demonstrate the feasibility of assessing image quality with large models. Remarkably, our IQAGPT outperforms GPT-4 and CLIP-IQA, as well as the multi-task classification and regression models that solely rely on images.

**Keywords:** Artificial intelligence, computed tomography (CT), large language model, vision-language model, ChatGPT, GPT-4, image quality assessment, subjective evaluation

## 1 Introduction

In recent years, there have been many advances in the field of large language models (LLMs), such as PaLM [1], LLaMA [2] and GPTs [3, 4, 5], which have shown excellent results in natural language processing (NLP) tasks including language translation, question answering, and text generation. The most remarkable breakthrough is ChatGPT, which is built upon InstructGPT [6] using labeler-written prompts and reinforcement learning from human feedback [7]. As a result, ChatGPT can produce

---

\*†: Co-first authors; ‡: Co-corresponding authors

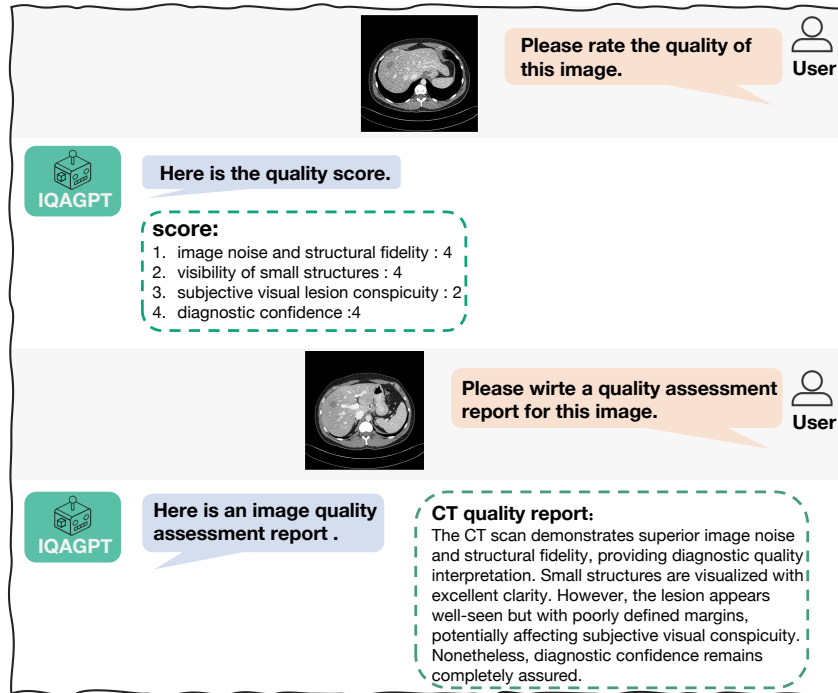


Figure 1: A dialogue between humans and the proposed IQAGPT. In the dialogues, IQAGPT can output scores and write the quality report based on an input image

more informative and human-like responses and interact quite naturally with users in a conversational manner, allowing it to help humans accomplish many tasks, such as writing and programming [8].

However, LLMs such as ChatGPT are unable to cope with visual information since they are only trained on textual data. To address this gap, visual-language models (VLMs) [9, 10, 11, 12, 13, 14, 15], which synergistically combine the capabilities of LLMs with visual processing, were proposed to capture rich vision-language correspondence and perform well in various multi-modal tasks such as report generation, diagnosis, and vision question answering. Recently, attempts have been made to interface LLMs, such as ChatGPT, with VLMs to understand visual information in computer vision tasks, leading to the development of multimodal models. In this context, OpenAI launched its new large vision-language model, GPT-4 [16], with amazing results on multimodal tasks during dialogues. Wu *et al.* [12] build a system, called Visual ChatGPT, by incorporating different vision models for users to interact with ChatGPT beyond language input. MiniGPT-4 [17] integrates an advanced large language model (LLM), Vicuna [18], and a pre-trained ViT [19] with a single linear projection layer, leading to a performance close to that of GPT-4.

While LLMs and VLMs are powerful in many tasks, up to now few efforts have been made to adapt them for image quality assessment (IQA), which plays an important role in imaging and image processing applications such as image restoration [20, 21, 22] and medical diagnosis [23, 24]. Particularly, in the field of computed tomography (CT), reconstructed low-dose CT images from various deep learning methods [25, 26, 27, 37, 28, 29, 30, 31] may lead to blurring or over-smoothing problems, hindering their clinical translation. Therefore, assessing CT image quality prior to diagnosis is essential. Over the past decades, several objective IQA metrics have been widely used, including peak signal-to-noise ratio (PSNR), structural similarity (SSIM), and root-mean-square error (RMSE). However, these metrics are neither well aligned with the subjective evaluations of radiologists nor with diagnostic accuracy.

Consequently, developing a medical image quality assessment system is highly desirable for radiologists to assess clinically relevant image quality such as lesion conspicuity. The most effective way is to invite experienced radiologists to review images [32] and give ground truth labels. However, this method is expensive and time-consuming. While several deep learning-based image quality assessment methods exist, they primarily focus on natural images with little linguistic interactiv-

ity. [33, 34, 35]. CLIP-IQA [36] utilizes a frozen CLIP model to calculate the similarity between images and predefined positive and negative prompts. Nevertheless, it was intended for natural images and can only train on simple text prompts, one metric each time. These limitations make it inadequate for complex medical IQA, particularly for evaluating small structures and lesions in CT images. An interesting question here we ask is: *Could we build a ChatGPT-like system based on VLMs to mimic the image quality evaluation by radiologists?*

In this paper, we propose an image quality assessment system with VLMs and ChatGPT, termed as IQAGPT. We build IQAGPT based on an image quality captioning VLM and incorporate it with ChatGPT to generate quality scores and summarize a quality report of CT images to be assessed. First, to train our IQAGPT, we collect a dataset of 1,000 image-text pairs, named CT-IQA, in which an experienced radiologist was asked to score CT images of different qualities similar to the subjective evaluation previously reported [32, 37], including image noise, small structures, lesion conspicuity, and diagnostic confidence. To utilize the strengths of LLMs in subjective image evaluation, we design a prompt template to convert the quality scores to text descriptions. Second, we develop an image quality captioning model built upon a pre-trained medical VLM [13] and fine-tune it on the CT-IQA dataset with an autoregressive language modeling objective that predicts the next token given the previous tokens [3]. Finally, through interacting with ChatGPT, IQAGPT can score CT images and generate quality reports based on the caption from the image quality captioning model. Figure 1 presents an exemplary dialogue between a user and the proposed IQAGPT.

In summary, the main contributions of this work are as follows.

- We introduce a hybrid large model approach for CT image quality assessment, which synergizes the objective and subjective image quality evaluation in a clinically important scenario.
- Specifically, we present an image quality assessment system consisting of VLMs and ChatGPT, termed IQAGPT, which is built on an image quality captioning model and can output quality scores and reports by interacting with ChatGPT.
- We collect a CT-IQA dataset for IQA, containing 1,000 image-text pairs professionally annotated according to four common subjective metrics used in diagnosis.
- Preliminary results demonstrate the feasibility of assessing CT image quality with IQAGPT, and the resulting text-guided image quality captioning model outperforms GPT-4 and CLIP-IQA.

## 2 Methods and Materials

The goal of this study is to develop an image quality assessment system with VLMs and ChatGPT, called IQAGPT. In the following, we first report on the CT-IQA dataset in Subsection 2.1. Then, in Subsections 2.2 and 2.3, we describe the image quality captioning model and our IQAGPT that interacts with ChatGPT, respectively. Furthermore, we give the implementation details in Subsection 2.4 and explain how we evaluate the performance of IQAGPT in Subsection 2.5.

### 2.1 CT-IQA Dataset

To adapt to the IQA task and achieve an accurate quality assessment of CT images, we created an image-text dataset called CT-IQA, in which an experienced radiologist was asked to assess CT images subjectively. To this end, we randomly selected normal-dose CT (NDCT) slices and corresponding low-dose CT images (LDCT) at 25% of the normal dose from the 2016 AAPM Grand Challenge dataset [38], which includes abdominal CT scans of 10 anonymous patients. Specifically, we selected 100 NDCT and LDCT pairs uniformly from 8 patients for training and 25 slice pairs uniformly from the remaining 2 patients for testing. Additionally, we randomly simulated some lesions in NDCT and corresponding LDCT to evaluate subjective visual lesion conspicuity. Next, we processed the selected 125 LDCT images with a modularized denoising model [37] called MAP-NN, which produced various intermediate denoised images with associated noise reduction directions. Besides, we implemented RED-CNN [25], a widely-used denoising model that was optimized with the MSE loss function. Finally, we obtained 1,000 CT slices with different quality, including 125 NDCT slices with corresponding 125 LDCT slices, 625 reconstructed images with 5 denoising levels from MAP-NN, and 125 reconstructed images from RED-CNN. We employed the abdomen window of all

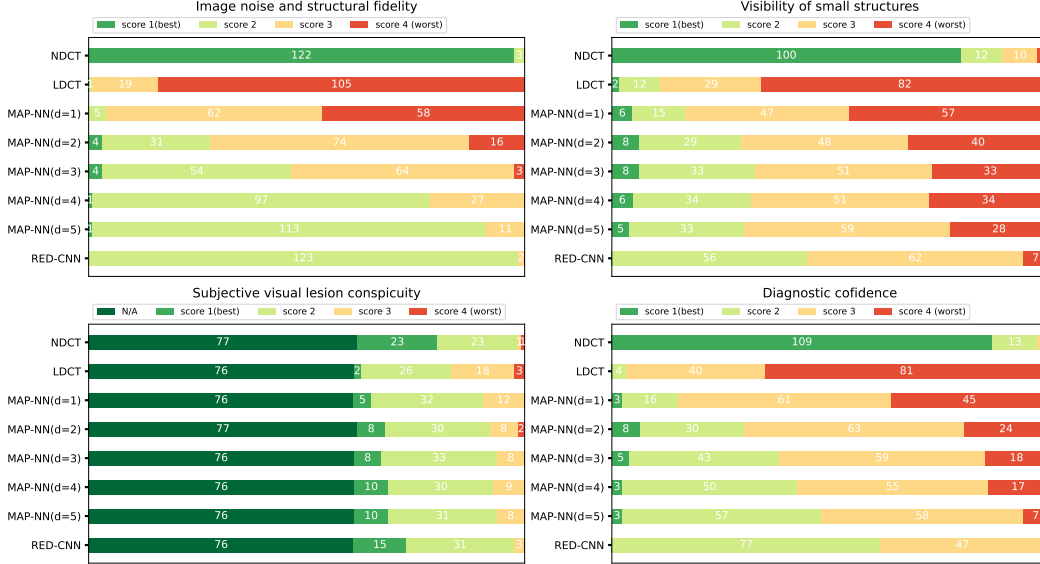


Figure 2: The distribution of scores of the four metrics assessed by the radiologist in constructing our CT-IQA dataset. Scores 1, 2, 3, and 4 are defined in Subsection 2.1.

CT scans [-160,240] HU for visualization of abdominal organs. The radiologist was asked to score these CT images in terms of four metrics used in the previous study [32, 37], which are defined as follows:

- Image noise and structural fidelity on a four-point scale (1 = Better than usual, acceptable for diagnostic interpretation; 2 = Average, acceptable for diagnostic interpretation; 3 = Sub-optimal, for limited diagnostic information only, 4= Unacceptable for diagnostic interpretation)
- The visibility of small structures (small blood vessels, adrenal glands, small lymph nodes) on a four-point scale (1 = excellent visualization, 2 = acceptable visibility, 3 = sub-optimal visibility, and 4 = unacceptable visualization)
- Subjective visual lesion conspicuity (N/A = if no lesion ) on a four-point scale (1 = well-seen lesion with well-visualized margins, 2 = well-seen lesion with poorly visualized margins, 3 = poorly seen lesion with poorly visualized margins, and 4 = lesion blurred with severe loss of margins)
- Diagnostic confidence on a four-point scale (1 = completely confident; 2 = probably confident; 3 = confident only for a limited clinical entity such as a kidney stone, a calcified lesion, or a large lesion; and 4 = poor confidence).

Figure 2 shows the distribution of human expert scores across the aforementioned four metrics for CT images of 8 different image qualities, including NDCT, LDCT, MAP-NN (d=1), MAP-NN (d=2), MAP-NN (d=3), MAP-NN (d=4), MAP-NN (d=5), and RED-CNN.  $d$  represents the denoising level.

## 2.2 Image Quality Captioning Model

Instead of using the rating scores to train a classification or regression model, we develop an image quality captioning model to summarize the image quality. By doing so, the vision language model with semantic text information and image-text fusion can better appreciate the subjective scores than image-only models, which will be further discussed in Section 3. Our model is based on a pre-trained medical VLM and fined-tuned with an autoregressive language modeling objective on the CT-IQA dataset. To leverage the capabilities of LLMs in the subjective image evaluation, we convert scores to quality descriptions using a specific prompt template during training. Our prompt template is defined as that “Image noise and structural fidelity: {description 1}; Visibility of small structures: {description 2}; Subjective visual lesion conspicuity: {description 3}; Diagnostic

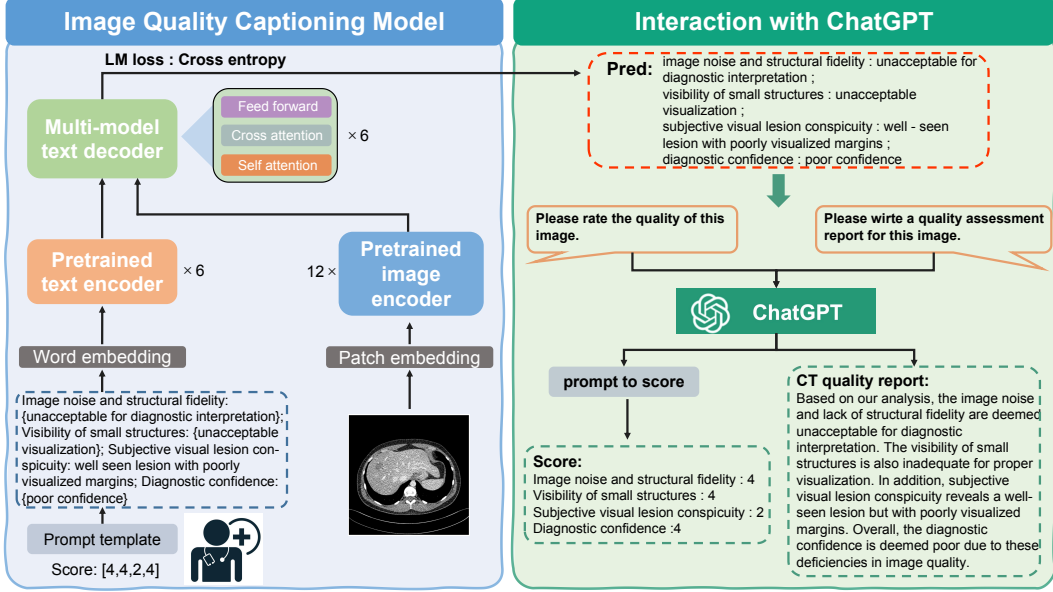


Figure 3: Overview of IQAGPT. While the left side shows our image quality captioning model, the right side details the process of the score and report generation through interacting with ChatGPT.

confidence: {description 4}”. Every description is the evaluation criterion corresponding to the score described in Subsection 2.1. An example to convert the score to the quality caption is given in the lower left part of Figure 3, where the score assessed by the radiologist is [4,4,2,4].

Our image quality captioning model consists of an image encoder, a text encoder, and a multi-modal text decoder, as shown on the left side of Figure 3. We use a 12-layer visual transformer ViT-S/16 [19] as the image encoder and the first 6 layers of the BERT<sub>base</sub> [39] model as the text encoder. The multi-modal text decoder is the last 6 layers of the BERT<sub>base</sub> to fuse image and the text features through cross-modal attention. The image encoder, text encoder, and multimodal decoder were pre-trained in radiography images and report pairs [13] using four learning objectives: contrastive learning for cross- and intra-modal alignment, masked language modeling for image-guided text completion, masked image modeling for text-guided image completion, and image-text matching; please refer to [13] for more details on these four objectives.

We fine-tuned the pre-trained models with the next word prediction to allow the auto-regressive generation of image captions for CT image quality assessment. We hypothesize that this paradigm, combined with our input template, allows LLMs to better comprehend the relationship between different metrics. We denote a CT-text pair as  $(I, T)$ , where  $I$  represents a CT slice and  $T$  is defined as  $T = (t_1, t_2, \dots, t_m)$  with  $m$  tokens. The objective is to maximize the following log-likelihood:

$$\mathcal{L}(I, T) = \sum_{i=1}^m \log P(t_i | t_1 : t_{i-1}, I; \theta), \quad (1)$$

where  $P$  is the conditional probability modeled by the image quality captioning model, and  $\theta$  represents the trainable parameters of the model.

### 2.3 Interaction with ChatGPT

ChatGPT provides a language interface with remarkable reasoning capabilities across many domains [12]. In our IQAGPT, we enable an interaction between ChatGPT and users, aimed at generating more comprehensive output information, as depicted on the right side of Figure 3. When a user uploads a CT image, they can prompt IQAGPT with a request like “Please rate the quality of this image.” or “Please write a quality assessment report for this image.” Subsequently, the user receives either a quality score or a detailed quality report. To this end, we use ChatGPT to perform corresponding operations on the output caption from the image quality captioning model. For the

score-related demands, it converts the predicted caption to the score according to the prompt template described in Subsection 2.1. For the report-related demands, it summarizes the predicted caption into a quality assessment report in a radiology report format.

## 2.4 Implementation Details

We trained our models with NVIDIA V100 GPUs. In the training process, we fine-tuned the image quality captioning model in IQAGPT for 50 epochs based on the pre-trained model [13], in which we used the AdamW optimizer [40] and the weight decay of 0.02. We initialized the learning rate at  $2.0 \times 10^{-4}$ , warm-up [41] in the first 2 epochs with the learning rate of  $1.0 \times 10^{-5}$ , and gradually reduced it to  $1.0 \times 10^{-6}$  with the cosine annealing [42]. For data processing, we employed the full-size images within an abdomen window of [-160, 240] HU and split 10 patients into the training and testing datasets by 8:2 as described in Subsection 2.1. Also, we randomly augmented training samples using horizontal flipping and rotation.

## 2.5 Evaluation Metrics

To show the effectiveness of IQAGPT, we quantitatively evaluated the performance of generated quality captioning and scores. First, we analyzed captioning results utilizing widely recognized metrics in text generation tasks: Bilingual Evaluation Understudy (BLEU-n; “n” means  $n$  words) [43], Recall Oriented Understudy of Gisting Evaluation (ROUGE-L; “L” means the longest common subsequence) [44], Metric for Evaluation of Translation with Explicit Ordering (METEOR) [45], and Consensus-based Image Description Evaluation (CIDEr; “r” stands for recall) [46]. These metrics measure the similarity between the generated and reference texts, with higher scores for better quality. Specifically, BLEU measures the quality of machine-translated text compared to a human reference translation. It computes an  $n$ -grams (phrases of  $n$  words) based precision for the candidate sentence with respect to the references. ROUGE-L focuses on the longest common subsequence between the evaluated text and the reference text. METEOR is based on the harmonic mean of unigram precision and recall, with recall weighted higher than precision. CIDEr measures the similarity of a generated sentence to a set of reference sentences by considering human consensus. Notably, BLEU-n, ROUGE-L, and METEOR scores range from 0 to 1 while CIDEr ranges from 0 to infinity. In addition, we converted the output text descriptions into scores, compared the performance in terms of accuracy as the classification evaluation, and computed the Pearson linear correlation coefficient (PLCC) and Spearman’s rank order correlation coefficient (SROCC) as the regression evaluation.

# 3 Results

## 3.1 Evaluation of Generated Quality Captioning

Table 1: Quantitative evaluation of captioning quality generated using IQAGPT and MiniGPT-4 respectively.

Method	BLEU-1	BLEU-2	BLEU-3	BLEU-4	METEOR	ROUGE-L	CIDEr
MiniGPT-4	0.798	0.733	0.717	0.652	0.516	0.826	3.070
<b>IQAGPT</b>	<b>0.819</b>	<b>0.777</b>	<b>0.742</b>	<b>0.712</b>	<b>0.546</b>	<b>0.858</b>	<b>3.620</b>

In Figure 4, we present two examples of our test results, where we converted the predicted descriptions to scores and quality reports using ChatGPT. It can be observed that IQAGPT consistently generates quality descriptions in excellent alignment with radiologists’ annotations. Furthermore, the reports generated using ChatGPT are consistent with the outputs from our quality captioning model, which effectively overcomes the limitations of the existing VLM dialogue when assessing the quality of medical images. Then, we compared the quantitative captioning performance of IQAGPT and MiniGPT-4, as depicted in Table 1. We did not employ GPT-4 [16], as its latest version, GPT-4V, is not tailored for interpreting specialized medical imagery such as CT scans. We fine-tuned the learnable linear layer in MiniGPT-4 using our CT-IQA dataset in their experimental settings [17]. IQAGPT achieves better quantitative results in seven metrics because the large language model (Vicuna [18]) in MiniGPT-4 lacks the expertise of CT quality assessment and it was frozen during



 <p style="text-align: right;">low-dose</p>	 <p style="text-align: right;">normal-dose</p>
<p><b>Ground-truth</b></p> <ol style="list-style-type: none"> <li>1. Image noise and structural fidelity : unacceptable for diagnostic interpretation;</li> <li>2. Visibility of small structures : unacceptable visualization;</li> <li>3. Subjective visual lesion conspicuity : no lesion;</li> <li>4. Diagnostic confidence : poor confidence</li> </ol>	<p><b>Ground-truth</b></p> <ol style="list-style-type: none"> <li>1. Image noise and structural fidelity : better than usual, acceptable for diagnostic interpretation;</li> <li>2. Visibility of small structures : acceptable visibility;</li> <li>3. Subjective visual lesion conspicuity: no lesion</li> <li>4. Diagnostic confidence : completely confident</li> </ol>
<p><b>Predicted</b></p> <ol style="list-style-type: none"> <li>1. Image noise and structural fidelity: unacceptable for diagnostic interpretation;</li> <li>2. Visibility of small structures: unacceptable visualization;</li> <li>3. Subjective visual lesion conspicuity: no lesion;</li> <li>4. Diagnostic confidence: poor confidence</li> </ol>	<p><b>Predicted</b></p> <ol style="list-style-type: none"> <li>1. Image noise and structural fidelity : better than usual, acceptable for diagnostic interpretation;</li> <li>2. Visibility of small structures: excellent visualization;</li> <li>3. Subjective visual lesion conspicuity: no lesion;</li> <li>4. Diagnostic confidence : completely confident</li> </ol>
<p><b>Rating by ChatGPT</b></p> <ol style="list-style-type: none"> <li>1. Image noise and structural fidelity: 4</li> <li>2. Visibility of small structures: 4</li> <li>3. Subjective visual lesion conspicuity: N/A</li> <li>4. Diagnostic confidence: 4</li> </ol>	<p><b>Rating by ChatGPT</b></p> <ol style="list-style-type: none"> <li>1. Image noise and structural fidelity: 1</li> <li>2. Visibility of small structures: 1</li> <li>3. Subjective visual lesion conspicuity: N/A</li> <li>4. Diagnostic confidence: 1</li> </ol>
<p><b>Report by ChatGPT</b></p> <p>The CT image reviewed exhibits unacceptable levels of image noise and structural fidelity, rendering it unsuitable for accurate diagnostic interpretation. Additionally, the visualization of small structures is inadequate, making it difficult to identify and analyze relevant anatomical features. No lesions are subjectively identified, but the image lacks any apparent visual lesion conspicuity. As a result of these limitations, diagnostic confidence is poor, and there is limited confidence in the accuracy of the imaging findings.</p>	<p><b>Report by ChatGPT</b></p> <p>The CT image under review exhibits better-than-usual image noise and structural fidelity, allowing for accurate diagnostic interpretation. The visibility of small structures is excellent, providing a clear visualization of the relevant anatomical features. No lesions are subjectively identified, and thus the image lacks any apparent visual lesion conspicuity. Overall, diagnostic confidence is high, and there is complete confidence in the accuracy of the imaging findings.</p>

Figure 4: The captions predicted using our method and ChatGPT’s generated scores and reports.

training. Consequently, while MiniGPT-4 was instable, our IQAGPT produced the quality description very consistent with radiologists’ annotations.

### 3.2 Evaluation of Generated Quality Score

To validate the efficacy of our image quality captioning model, we employed our prompt template that transforms output text descriptions into scores for assessing IQAGPT’s performance in both the classification and regression tasks. Specifically, we conducted a comparative study on IQAGPT with an image-only multi-task classification model, using accuracy as a metric. Additionally, IQAGPT was compared against CLIP-IQA [36] and an image-only multi-task regression model, employing PLCC and SROCC. These quantitative results are detailed in Tables 2 and 3. It is pertinent to note that CLIP-IQA+ represents the fine-tuned version of CLIP-IQA. The calculation of PLCC and SROCC for the metric of subjective visual lesion conspicuity was not performed, as over half of the CT scans in our dataset do not contain lesions. For the image-only multi-task classification and regression models, we name them ViT-C and ViT-R respectively. First, we utilized the same pre-trained image encoder (ViT-S/16) in IQAGPT to extract image features. Then, four pairs of fully-connected layers were implemented following the classification (CLS) token for four metrics, as depicted in Figure 5. The ViT-C and ViT-R employed cross-entropy loss and mean squared error loss respectively. We used the same training strategy with IQAGPT for training CLIP-IQA+, ViT-C, and ViT-R.

In Table 2, it is evident that IQAGPT outperformed the image-only classification model ViT-C across four metrics, achieving a notable improvement of 0.19 in mean accuracy. For regression, IQAGPT surpassed CLIP-IQA, as shown tasks in Table 3. In addition, a notable advantage of IQAGPT is its efficiency; unlike CLIP-IQA, which requires separate fine-tuning for each of the four metrics, IQAGPT is capable of simultaneously producing results for all metrics as a single output.

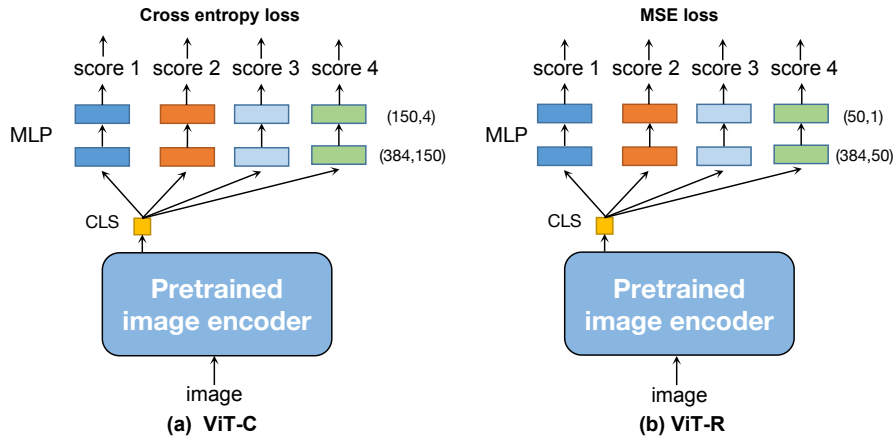


Figure 5: The flowcharts of (a) the multi-task classification model ViT-C and (b) the multi-task regression model ViT-R, respectively. CLS Tokens are followed by four groups of classifiers, each consisting of two fully-connected layers. Scores 1, 2, 3, and 4 are the categories corresponding to the four metrics described in Subsection 2.1.

Table 2: Performance comparison of IQAGPT with ViT-C in the classification evaluation in terms of accuracy.

	ViT-C	IQAGPT
Image noise and structural fidelity	0.545	<b>0.765</b>
Visibility of small structures	0.405	<b>0.620</b>
Subjective visual lesion conspicuity	0.725	<b>0.820</b>
Diagnostic confidence	0.375	<b>0.605</b>
Mean	0.512	<b>0.702</b>

Table 3: Performance comparison of IQAGPT with CLIP-IQA and ViT-R in the regression evaluation in terms of PLCC and SROCC (PLCC/SROCC).

	CLIP-IQA	CLIP-IQA+	ViT-R	IQAGPT
Image noise and structural fidelity	0.277/0.271	0.742/0.633	0.580/0.460	<b>0.821/0.820</b>
Visibility of small structures	0.121/0.117	0.712/0.696	0.436/0.415	<b>0.743/0.735</b>
Subjective visual lesion conspicuity	-	-	-	-
Diagnostic confidence	0.081/0.069	0.650/0.642	0.504/0.422	<b>0.699/0.689</b>
Mean	0.160/0.114	0.701/0.657	0.531/0.519	<b>0.754/0.748</b>

Table 4: Accuracy for each of four metrics in eight image quality levels. Metric 1: Image noise and structural fidelity; Metric 2: Visibility of small structures; Metric 3: Subjective visual lesion conspicuity; and Metric 4: Diagnostic confidence. MAP-NN( $\cdot$ ) provides 5 denoising levels [37].

	NDCT	LDCT	MAP-NN(1)	MAP-NN(2)	MAP-NN(3)	MAP-NN(4)	MAP-NN(5)	RED-CNN	Mean
Metric 1	1.000	0.800	0.600	0.520	0.480	0.880	0.880	1.000	0.765
Metric 2	0.960	0.680	0.480	0.360	0.520	0.600	0.640	0.720	0.620
Metric 3	0.920	0.920	0.880	0.760	0.800	0.840	0.760	0.800	0.820
Metric 4	0.920	0.760	0.360	0.400	0.320	0.440	0.680	0.960	0.605
Mean	0.950	0.790	0.580	0.510	0.520	0.690	0.740	0.840	0.702



For each image quality level and metric, we computed accuracy using converted scores, as depicted in Table 4. The relative accuracies associated with intermediate images generated by MAP-NN may not be highly robust, due to their similar image features. This aligns with the challenges in the subjective evaluation of images with subtle quality differences, a critical aspect of our CT-IQA dataset. Our study highlights the complexity of differentiating between similar images.

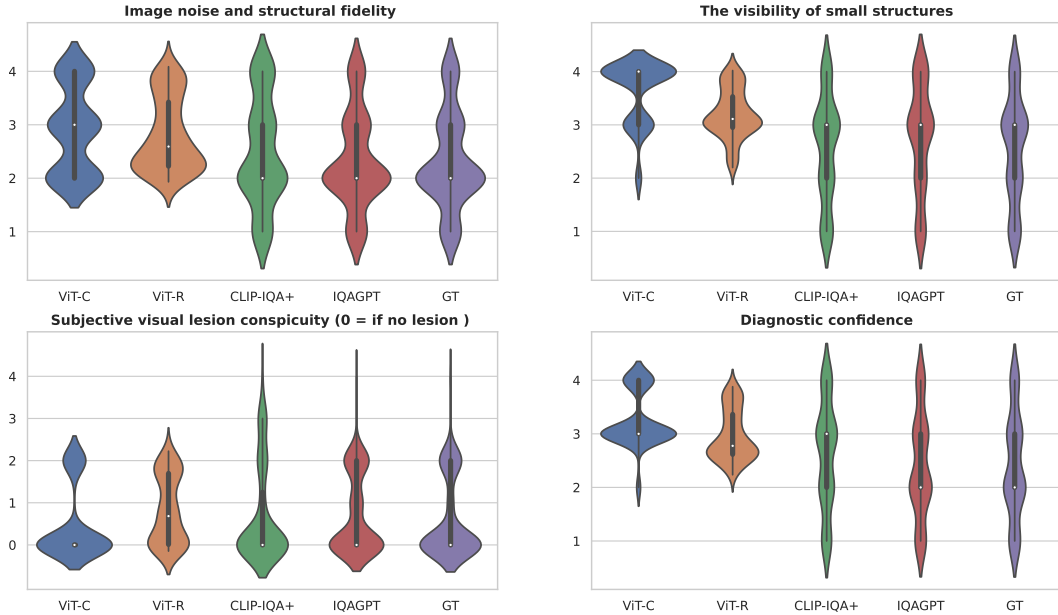


Figure 6: Scores distribution for four quality metrics using IQAGPT, ViT-C, ViT-R, and CLIP-IQA+. The last column lists the ground-truth (GT) scores.

Furthermore, we present the score distributions of IQAGPT, ViT-C, ViT-R, and CLIP-IQA+ for four quality metrics in Figure 6. Notably, our method more closely approximates the ground truth compared to ViT-C, ViT-R, and CLIP-IQA+, demonstrating its effectiveness. Overall, our method has a higher correlation with human perception than the competing methods, marking a significant advancement in CT subjective image quality assessment.

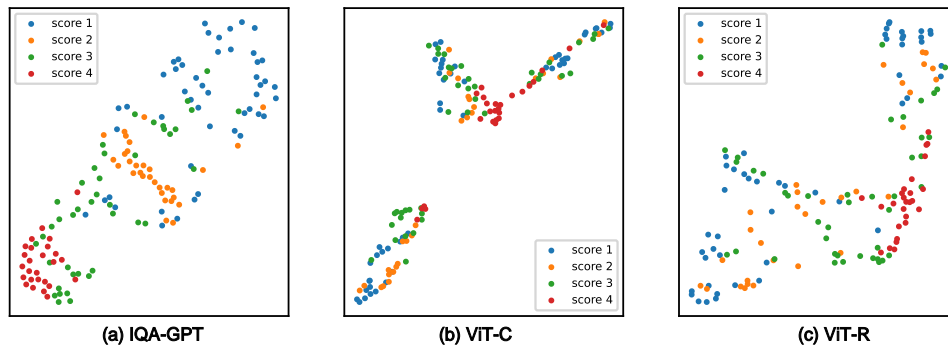


Figure 7: Feature visualization of the CLS token in the image encoder of (a) IQAGPT, (b) ViT-C, and (c) ViT-R, using the t-SNE method. The samples are labeled with categories from the metric of “Image noise and structural fidelity”.

### 3.3 Ablation on LLMs

To further demonstrate the effectiveness of textual semantic information, we employed the *t*-SNE [47] method to visualize the features of the CLS token in the image encoders of IQAGPT, ViT-C, and ViT-R, as illustrated in Figure 7. Each sample was labeled using the score of the “Image noise

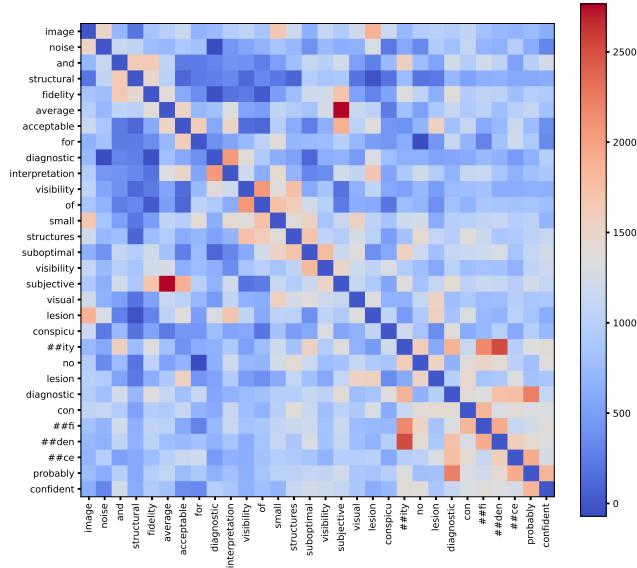


Figure 8: The self-attention map of tokens from the last layer in the multi-modal text decoder.

and structural fidelity” metric. This visualization demonstrates that IQAGPT distinguished features of different categories more clearly than ViT-C and ViT-R, and exhibiting an ordered sequence in the score-based feature representation. Additionally, the self-attention map of tokens from the multi-modal text decoder, depicted in Figure 8, reveals that each token is interconnected not only with tokens from the same task but also with those from preceding tasks. This finding underscores the merits of textual descriptions in capturing inter-task correlations, thereby enhancing the classification performance.

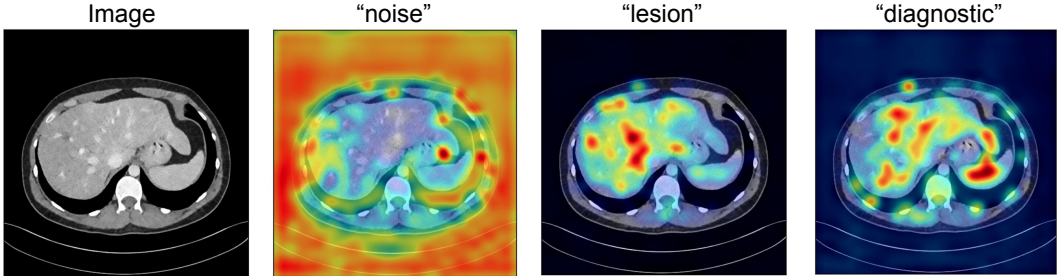


Figure 9: Grad-CAM visualizations on the cross-attention maps corresponding to individual words.

### 3.4 Interpretation

To provide an interpretation of our quality captioning model, we present the per-word Grad-CAM visualizations in Figure 9. It can be seen that the Grad-CAM visualizations are highly correlated with where radiologists would look at when making decisions. For instance, radiologists tend to concentrate on the global appearance of an image when assessing “noise”, whereas local features gain more attention during evaluations of “diagnosis” or “lesions”.

Overall, the above findings indicate that our IQAGPT is capable of successfully performing the CT subjective quality assessment task. It can not only predict texts aligned with the ground truth but also translate these predictions into scores and reports through ChatGPT in a clinically meaningful way.

## 4 Discussion

Our study highlights the efficacy of integrating large models for image quality assessment, with a specific focus on low-dose CT denoising. It suggests a significant potential to replace a traditional subjective image quality evaluation procedure conducted by radiologists with a large hybrid deep model, which would be resource-efficient and time-saving. In other words, our developed IQAGPT has made the first attempt along this direction, and IQAGPT not only eases the burden on radiologists by automating CT image quality assessment but also promises to aid radiologists in refining the diagnostic performance.

Our method was developed on a CT-IQA dataset of 1,000 image-text pairs annotated by a professional radiologist. For this purpose, we leveraged a prompt template to transform quality scores into text descriptions. Having fine-tuned an image quality captioning model on CT-IQA dataset, IQAGPT can generate quality descriptions for different CT scans. The utilization of ChatGPT as an interactive interface facilitates user engagement, allowing for versatile outputs including quality scores and comprehensive reports.

Our experimental results demonstrate the efficacy of IQAGPT, which can generate quality descriptions steadily and convert them to scores and reports successfully. Our quantitative evaluation, using metrics for image captioning, classification, and regression tasks, underscores its superior performance. In addition, our ablation study shows the effectiveness of incorporating LLMs in subjective CT IQA tasks because it can integrate the expertise of radiologists with the advanced capabilities of LLMs. Furthermore, LLM provides an interpretation of generated results using the quality captioning model. Note that while CLIP-IQA also employs LLMs, its limitation to training one metric at a time with simple text prompts restricts its applicability in complex medical IQA scenarios, especially when assessing fine structures and small lesions.

However, our work also has some limitations, which open avenues for enhancements. Currently, our study is based on a relatively small dataset annotated by a single radiologist. Expanding this dataset will likely enhance the accuracy and reliability of our model, potentially making IQAGPT a new standard for medical image quality assessment. Additionally, more interactive elements between radiologists and the model would be beneficial such as tracking radiologists' eyes. Future work might include a text-guided denoising model, allowing radiologists to refine poor-quality images and improve radiology reports.

## 5 Conclusion

In conclusion, our study presents a pioneering exploration into CT subjective quality assessment, utilizing an innovative amalgamation of vision-language models and ChatGPT. We collect CT-IQA, an image-text dataset comprising pairs of CT scans with quality scores annotated by an experienced radiologist. We develop IQAGPT, fine-tuned on a vision-language model using the CT-IQA dataset, which can integrate with ChatGPT to generate both quality scores and detailed reports. The extensive experimental results not only demonstrate the feasibility of IQAGPT but also highlight the effectiveness of LLMs, marking a significant potential in the field of subjective image quality assessment integrated with LLMs.

## References

- [1] Aakanksha Chowdhery, Sharan Narang, Jacob Devlin, Maarten Bosma, Gaurav Mishra, Adam Roberts, Paul Barham, Hyung Won Chung, Charles Sutton, Sebastian Gehrmann, et al. PaLM: Scaling language modeling with pathways. *arXiv preprint arXiv:2204.02311*, 2022.
- [2] Hugo Touvron, Thibaut Lavril, Gautier Izacard, Xavier Martinet, Marie-Anne Lachaux, Timothée Lacroix, Baptiste Rozière, Naman Goyal, Eric Hambro, Faisal Azhar, et al. LLaMA: Open and efficient foundation language models. *arXiv preprint arXiv:2302.13971*, 2023.
- [3] Alec Radford, Karthik Narasimhan, Tim Salimans, Ilya Sutskever, et al. Improving language understanding by generative pre-training. *OpenAI blog*, 2018.
- [4] Alec Radford, Jeffrey Wu, Rewon Child, David Luan, Dario Amodei, Ilya Sutskever, et al. Language models are unsupervised multitask learners. *OpenAI blog*, 1(8):9, 2019.

- [5] Tom Brown, Benjamin Mann, Nick Ryder, Melanie Subbiah, Jared D Kaplan, Prafulla Dhariwal, Arvind Neelakantan, Pranav Shyam, Girish Sastry, Amanda Askell, et al. Language models are few-shot learners. *NeurIPS*, 33:1877–1901, 2020.
- [6] Long Ouyang, Jeffrey Wu, Xu Jiang, Diogo Almeida, Carroll Wainwright, Pamela Mishkin, Chong Zhang, Sandhini Agarwal, Katarina Slama, Alex Ray, et al. Training language models to follow instructions with human feedback. *NeurIPS*, 35:27730–27744, 2022.
- [7] Paul F Christiano, Jan Leike, Tom Brown, Miljan Martic, Shane Legg, and Dario Amodei. Deep reinforcement learning from human preferences. *NeurIPS*, 30, 2017.
- [8] Mark Chen, Jerry Tworek, Heewoo Jun, Qiming Yuan, Henrique Ponde de Oliveira Pinto, Jared Kaplan, Harri Edwards, Yuri Burda, Nicholas Joseph, Greg Brockman, et al. Evaluating large language models trained on code. *arXiv preprint arXiv:2107.03374*, 2021.
- [9] Wenhui Wang, Hangbo Bao, Li Dong, Johan Bjorck, Zhiliang Peng, Qiang Liu, Kriti Aggarwal, Owais Khan Mohammed, Saksham Singhal, Subhojit Som, et al. Image as a foreign language: BEiT pretraining for vision and vision-language tasks. In *CVPR*, pages 19175–19186, 2023.
- [10] Junnan Li, Dongxu Li, Silvio Savarese, and Steven Hoi. BLIP-2: Bootstrapping language-image pre-training with frozen image encoders and large language models. *arXiv preprint arXiv:2301.12597*, 2023.
- [11] Danny Driess, Fei Xia, Mehdi SM Sajjadi, Corey Lynch, Aakanksha Chowdhery, Brian Ichter, Ayzaan Wahid, Jonathan Tompson, Quan Vuong, Tianhe Yu, et al. PaLM-E: An embodied multimodal language model. *arXiv preprint arXiv:2303.03378*, 2023.
- [12] Chenfei Wu, Shengming Yin, Weizhen Qi, Xiaodong Wang, Zecheng Tang, and Nan Duan. Visual ChatGPT: Talking, drawing and editing with visual foundation models. *arXiv preprint arXiv:2303.04671*, 2023.
- [13] Sangjoon Park, Eun Sun Lee, Kyung Sook Shin, Jeong Eun Lee, and Jong Chul Ye. Self-supervised multi-modal training from uncurated image and reports enables zero-shot oversight artificial intelligence in radiology. *arXiv preprint arXiv:2208.05140*, 2023.
- [14] Chuang Niu and Ge Wang. CT multi-task learning with a large image-text (LIT) model. *arXiv preprint arXiv:2304.02649*, 2023.
- [15] Qing Lyu, Josh Tan, Michael E Zapadka, Janardhana Ponnatapura, Chuang Niu, Kyle J Myers, Ge Wang, and Christopher T Whitlow. Translating radiology reports into plain language using ChatGPT and GPT-4 with prompt learning: results, limitations, and potential. *Vis. Comput. Ind. Biomed. Art.*, 6(1):9, 2023.
- [16] OpenAI. Gpt-4 technical report, 2023.
- [17] Deyao Zhu, Jun Chen, Xiaoqian Shen, Xiang Li, and Mohamed Elhoseiny. MiniGPT-4: Enhancing vision-language understanding with advanced large language models. *arXiv preprint arXiv:2304.10592*, 2023.
- [18] Wei-Lin Chiang, Zhuohan Li, Zi Lin, Ying Sheng, Zhanghao Wu, Hao Zhang, Lianmin Zheng, Siyuan Zhuang, Yonghao Zhuang, Joseph E Gonzalez, et al. Vicuna: An open-source chatbot impressing GPT-4 with 90%\* ChatGPT quality. See <https://vicuna.lmsys.org> (accessed 14 April 2023), 2023.
- [19] Alexey Dosovitskiy et al. An image is worth 16x16 words: Transformers for image recognition at scale. In *ICLR*, 2020.
- [20] Mriganka Sarmah, Arambam Neelima, and Heisnam Rohen Singh. Survey of methods and principles in three-dimensional reconstruction from two-dimensional medical images. *Vis. Comput. Ind. Biomed. Art.*, 6(1):15, 2023.
- [21] Jed D Pack, Mufeng Xu, Ge Wang, Lohendran Baskaran, James Min, and Bruno De Man. Cardiac CT blooming artifacts: clinical significance, root causes and potential solutions. *Vis. Comput. Ind. Biomed. Art.*, 5(1):1–13, 2022.
- [22] Yiming Lei, Chuang Niu, Junping Zhang, Ge Wang, and Hongming Shan. CT image denoising and deblurring with deep learning: Current status and perspectives. *IEEE Trans. Radiat. Plasma Med. Sci.*, 2023.
- [23] Chuang Niu and Ge Wang. Advances in deep learning techniques for biomedical imaging. *Vis. Comput. Ind. Biomed. Art.*, 6(1):1–2, 2023.

- [24] Khalid Al-Hammuri, Fayez Gebali, Awos Kanan, and Ilamparithi Thirumarai Chelvan. Vision transformer architecture and applications in digital health: a tutorial and survey. *Vis. Comput. Ind. Biomed. Art.*, 6(1):14, 2023.
- [25] Hu Chen, Yi Zhang, Mannudeep K Kalra, Feng Lin, Yang Chen, Peixi Liao, Jiliu Zhou, and Ge Wang. Low-dose CT with a residual encoder-decoder convolutional neural network. *IEEE Trans. Med. Imaging*, 36(12):2524–2535, 2017.
- [26] Qingsong Yang, Pingkun Yan, Yanbo Zhang, Hengyong Yu, Yongyi Shi, Xuanqin Mou, Mannudeep K Kalra, Yi Zhang, Ling Sun, and Ge Wang. Low-dose CT image denoising using a generative adversarial network with Wasserstein distance and perceptual loss. *IEEE Trans. Med. Imaging*, 37(6):1348–1357, 2018.
- [27] Hongming Shan, Yi Zhang, Qingsong Yang, Uwe Kruger, Mannudeep K Kalra, Ling Sun, Wenxiang Cong, and Ge Wang. 3-D convolutional encoder-decoder network for low-dose CT via transfer learning from a 2-D trained network. *IEEE Trans. Med. Imaging*, 37(6):1522–1534, 2018.
- [28] Lin Fu and Bruno De Man. Deep learning tomographic reconstruction through hierarchical decomposition of domain transforms. *Vis. Comput. Ind. Biomed. Art.*, 5(1):1–13, 2022.
- [29] Qi Gao, Zilong Li, Junping Zhang, Yi Zhang, and Hongming Shan. CoreDiff: Contextual error-modulated generalized diffusion model for low-dose CT denoising and generalization. *IEEE Trans. Med. Imaging*, 2023.
- [30] Zhihao Chen, Qi Gao, Yi Zhang, and Hongming Shan. ASCON: Anatomy-aware supervised contrastive learning framework for low-dose ct denoising. In *MICCAI*, pages 355–365. Springer, 2023.
- [31] Zhihao Chen, Chuang Niu, Ge Wang, and Hongming Shan. LIT-Former: Linking in-plane and through-plane transformers for simultaneous CT image denoising and deblurring. *arXiv preprint arXiv:2302.10630*, 2023.
- [32] Sarabjeet Singh, Mannudeep K Kalra, Jiang Hsieh, Paul E Licato, Synho Do, Homer H Pien, and Michael A Blake. Abdominal CT: comparison of adaptive statistical iterative and filtered back projection reconstruction techniques. *Radiology*, 257(2):373–383, 2010.
- [33] Pavan C Madhusudana, Neil Birkbeck, Yilin Wang, Balu Adsumilli, and Alan C Bovik. Image quality assessment using synthetic images. In *WACV*, pages 93–102, 2022.
- [34] Pavan C Madhusudana, Neil Birkbeck, Yilin Wang, Balu Adsumilli, and Alan C Bovik. CONVIQT: Contrastive video quality estimator. *IEEE Trans. Image Process.*, 2023.
- [35] Qi Gao, Sui Li, Manman Zhu, Danyang Li, Zhaoying Bian, Qingwen Lyu, Dong Zeng, and Jianhua Ma. Blind CT image quality assessment via deep learning framework. In *NSS/MIC*, pages 1–4. IEEE, 2019.
- [36] Jianyi Wang, Kelvin CK Chan, and Chen Change Loy. Exploring CLIP for assessing the look and feel of images. In *AAAI*, volume 37, pages 2555–2563, 2023.
- [37] Hongming Shan, Atul Padole, Fatemeh Homayounieh, Uwe Kruger, Ruhani Doda Khera, Chayanin Nitiwarangkul, Mannudeep K Kalra, and Ge Wang. Competitive performance of a modularized deep neural network compared to commercial algorithms for low-dose CT image reconstruction. *Nat. Mach. Intell.*, 1(6):269–276, 2019.
- [38] Cynthia H McCollough, Adam C Bartley, Rickey E Carter, Baiyu Chen, Tammy A Drees, Phillip Edwards, David R Holmes III, Alice E Huang, Farhana Khan, Shuai Leng, et al. Low-dose CT for the detection and classification of metastatic liver lesions: results of the 2016 low dose CT grand challenge. *Med. Phys.*, 44(10):e339–e352, 2017.
- [39] Jacob Devlin, Ming-Wei Chang, Kenton Lee, and Kristina Toutanova. BERT: Pre-training of deep bidirectional transformers for language understanding. In *NAACL*, pages 4171–4186, June 2019.
- [40] Ilya Loshchilov and Frank Hutter. Decoupled weight decay regularization. In *ICLR*, 2019.
- [41] Priya Goyal et al. Accurate, large minibatch SGD: Training ImageNet in 1 hour. *arXiv preprint arXiv:1706.02677*, 2017.
- [42] Ilya Loshchilov and Frank Hutter. SGDR: Stochastic gradient descent with warm restarts. In *ICLR*, 2017.

- [43] Kishore Papineni, Salim Roukos, Todd Ward, and Wei-Jing Zhu. BLEU: a method for automatic evaluation of machine translation. In *ACL*, pages 311–318, 2002.
- [44] Chin-Yew Lin. ROUGE: A package for automatic evaluation of summaries. In *Text Summ. Branch. Out*, pages 74–81, 2004.
- [45] Satanjeev Banerjee and Alon Lavie. METEOR: An automatic metric for MT evaluation with improved correlation with human judgments. In *ACL Workshop*, 2005.
- [46] Ramakrishna Vedantam, C Lawrence Zitnick, and Devi Parikh. CIDEr: Consensus-based image description evaluation. In *CVPR*, pages 4566–4575, 2015.
- [47] Laurens Van der Maaten and Geoffrey Hinton. Visualizing data using t-SNE. *J. Mach. Learn. Res.*, 9(11), 2008.